

## THE IMPACT OF THE GAS TURBINE BLADE HEATING TEMPERATURE IN THE PRESENCE OF AVIATION KEROSENE ON COATING AND ALLOY MICROSTRUCTURE

Mariusz BOGDAN\*<sup>ORCID</sup>, Artur KUŁASZKA\*\*<sup>ORCID</sup>, Dariusz ZASADA\*\*\*<sup>ORCID</sup>

\*Faculty of Mechanical Engineering, Białystok Technical University, 45 Wiejska Street, 15-333 Białystok, Poland

\*\*Air Force Institute of Technology, 6 Księcia Bolesława Street, 01-494 Warsaw, Poland

\*\*\*Faculty of Advanced Technologies and Chemistry, Military University of Technology, 2 Kaliskiego Street, 00-908 Warszawa, Poland

[m.bogdan@pb.edu.pl](mailto:m.bogdan@pb.edu.pl), [artur.kulaszka@itwl.pl](mailto:artur.kulaszka@itwl.pl), [dariusz.zasada@wat.edu.pl](mailto:dariusz.zasada@wat.edu.pl)

received 15 July 2024, revised 30 October 2024, accepted 30 November 2024

**Abstract:** Under operating conditions, gas turbine blades may experience overheating. The degree of unfavourable modifications of the condition of both the protective insulating coating and the alloy (microstructure degradation) depends, among other factors, on the temperature and its exposure time. In this study, under laboratory conditions, in the presence of aviation kerosene exhaust gases, the influence of temperature (mainly outside the range of nominal operating temperatures) on the condition of uncooled polycrystalline rotor blades of aircraft turbine jet engines was examined. The object of the research were new gas turbine blades of the SO-3 aircraft engine made of the EI-867 WD alloy, which were exposed to high temperatures for a period of two hours in a laboratory furnace in the temperature range  $T = 1123 - 1523\text{K}$ , every 100K. The article determines the nature of changes (modifications) both in the state of the coatings and in the core material (alloy). A multifactor analysis was taken into account, including in the case of coatings modifications: morphological microstructure of the coating, chemical composition of oxides and roughness parameters, and in the case of the alloy mainly grain growth, and modification of the strengthening  $\gamma'$  phase. As a result of exposure to high temperatures in the surroundings of exhaust gases, the roughness of the surface changes and various types of oxides are formed, and its thickness increases. An increasing number of carbides appeared in the EI-867 WD alloy and grain growth was found as a function of the heating temperature. In particular, the blade alloy structure experienced the growth of the reinforcing  $\gamma'$  phase, which is adverse in terms of heat resistance, and the percentage-wise depletion of this phase in the alloy structure. Due to the aforementioned changes, heated blades experiences significant reduction in heat resistance and high-temperature creep resistance. The article also indicates the possibility of using the characteristics of microstructural changes to determine the technical condition of the tested turbine element in a non-destructive way.

**Key words:** gas turbine blade, temperature, coating structure, alloy structure

### 1. INTRODUCTION

In aviation, the gas turbine has found wide application due to the relatively high efficiency of the energy conversion process, amounting to 30-45%. Its most important feature is the high operating temperature of the blades. Nickel-based superalloys are widely used due to their particular combination of very good mechanical properties and good structural stability at high temperatures [1÷3]. However, increasing the operating temperature of blades made of nickel superalloys is limited. This is due to the barrier of reducing the heat resistance of the superalloy in the presence of high exhaust gas temperature. A number of measures are taken to reduce the temperature of the blade superalloy, such as allowing internal cooling and applying coatings [4÷11].

During the operation of gas turbine blades, and especially the rotor blades of the manoeuvring aircraft engine, the blades are subjected to complex stress and thermal loads, as well as oxidation and hot corrosion processes. Extreme and complex operating conditions of the blades may intensify the basic destructive processes, which mainly include: creep, overheating and melting, corrosion and fatigue cracking, intergranular and thermal corrosion, low- and high-cycle fatigue: thermal and thermo-mechanical, erosion, and burnout [13÷16]. Among the factors that degrade the

blades, high operating temperature is of particular importance, as it rapidly accelerates the diffusion processes taking place in the blades. Under operating conditions, an excessive increase in exhaust gas temperature, which has a long-term effect, has a destructive effect on the technical condition of the blades [17÷22]. It is closely related to the material criterion, because the strength properties of superalloys are an appropriate microstructure that is not subject to weakening changes during operation, which is the main criterion for the durability of gas turbine blades [1, 3, 22÷26].

The process of destruction of blades during operation begins with the destruction of the coating, which is the first barrier of "contact" of exhaust gases (high temperature, pressure, chemical interaction) with the blade surface. High-temperature, highly oxidizing environments contain large amounts of chemical impurities. Therefore, heat-resistant coatings are mainly characterized by high resistance to high-temperature corrosion in a gaseous environment. Other features include low thermal conductivity and high structural stability [8, 11, 17]. To protect blades made of nickel alloys, mainly heat-resistant coatings made of metal alloys are used: (Ni, Co)-Cr-Al-Y or Al-Si-Ni-Y. Among the aluminium compounds that are created during the coating process, the intermetallic phase  $\beta$ -(NiAl) turns out to be the best compromise because it is a very good mix of mechanical properties and is characterized by high resistance to high temperatures [8, 11, 17]. In order to increase the thermal stability of this phase, the

composition of the covering material is supplemented with alloy additives. Under operating conditions, a layer of aluminium oxides  $Al_2O_3$  is formed on the surface of the  $\beta$ -NiAl layer, significantly reducing the oxidation rate. Degradation of the coatings occurs as a result of diffusion processes causing oxidation and an increase in the thickness of the oxide layer, as well as the progressive burning of alloy additions from the coating material, which impairs the self-regeneration capabilities of the coating (healing of micro-damages). Depletion of the covering material may also be caused by the diffusion of alloy additives into the substrate [4, 11, 27].

Assessment of the technical condition of turbine blades is a very important aspect in the process of operating aircraft turbine engines and is carried out using various techniques and methods [28, 29]. One of the techniques developed by M. Bogdan et al. [30-32] is the possibility of assessing or computer-aided assessment of the technical condition of the blades based on operational colour changes of the blade coating surface.

In this context, one of the main goals of this work was to describe the structural changes in both the coating and the alloy, reflecting a significant deterioration in the technical condition of the test object defined on the basis of the material criterion. This approach is important for specifying the procedure of the proposed non-destructive testing (NDT) for operational blades.

The article examined in laboratory conditions the influence of increased temperature (outside the nominal operating range of the blades) on the modification of the alloy material as well as the condition of the coating of the blades made of the EI-867 WD alloy with a diffusion-applied aluminized coating. In section 2, the research object (the method of its production and selected features) and the implementation of the experiment were characterized. Section 3 specifies the changes occurring in the coating in terms of changes in surface roughness, its chemical composition, morphological structure and coating thickness. Section 4 draws attention to selected aspects related to the change of the alloy structure. Changes in grain size, carbide precipitates and the strengthening  $\gamma'$  phase were determined. Section 5 discusses the test results in the context of linking material changes in the blades with the deterioration of strength properties. In section 6, practical implications of the findings and their limitations are outlined. The final part of the article contains final conclusions.

## 2. CHARACTERISTICS OF THE TESTED OBJECT AND DESCRIPTION OF THE EXPERIMENT

A set of new blades (Fig. 1) from one production batch was used for laboratory tests. Five blades were exposed to temperatures ranging from 1123K to 1523K, every 100K, by heating them for two hours in an FCF 60 chamber furnace filled with continuously generated aviation kerosene exhaust gases. Cooling took place in the furnace. The heating time and temperature affect both coagulation and the growth kinetics of  $\gamma'$  phase particles, as well as modifying the thickness of the blade's protective coating. The duration of temperature exposure was selected experimentally based on the results of the analysis of data obtained from the operational flight parameter recorder of the Ts-11 Iskra training aircraft (with an SO-3W turbojet engine installed). The profile of the flights performed and the engine service life of 400 hours were taken into account. Additionally, based on the metallographic tests carried out, it was found that the differences between heating for 2 hours and 3 hours at a temperature above the maximum

temperature after the turbine, i.e. 1323 K, do not significantly affect the change in the coating thickness or the average particle size of the  $\gamma'$  phase.



Fig. 1. Example of blade convex (suction face) surfaces

The EI-867 WD alloy is characterized by a structure typical of nickel superalloys. It consists of carbides,  $\gamma$  phase and  $\gamma'$  reinforcing phase and borides. The  $\gamma$  phase is a solid solution in nickel elements such as chromium, molybdenum, aluminium, cobalt and tungsten. The relative volume of the  $\gamma'$  phase ( $Ni_3Al$ ), which takes the shape of cubic particles, does not exceed 31–34%. The distinguishing feature is that the EI-867 WD alloy (chemical composition given in Tab. 1) does not contain titanium. In addition, it is characterized by a lower chromium content compared to other superalloys, which translates into greater susceptibility to corrosion. Therefore, elements made of these alloys require protective and insulating coatings. They are produced using thermochemical treatment, i.e. in the aluminization process. Aluminizing is carried out using the out-of-pack method at a temperature of 1223 K and for 12 hours.

Tab 1. Chemical composition of the superalloy used in the present study (wt.%)

C	Mn	Si	Cr	Co	Mo	W	Al	B	Fe	Ni
max	max	max						max		Rest
0.1	0.3	0.6	9.0	14.0	10.3	5.0	4.5	0.02	4.0	

The desired properties of the alloy (increase in mechanical strength, yield strength with increasing temperature, corrosion resistance required in special, demanding working conditions) are formed in a complex technological process of alloy production and include heat treatment involving precipitation hardening. Heat treatment includes supersaturation and aging. Supersaturation takes place at a temperature of  $1473 \pm 283$  K for 4 to 6 hours, causing the dissolution of some carbides and intermetallic phases in the matrix. Cooling in air during supersaturation leads to the separation of small particles of the  $\gamma'$  phase, the relative volume of which is approximately 20%. The aging process affects the further secretion of  $\gamma'$  phase particles and the growth of previously isolated particles. Among the carbides whose relative volume in the alloy does not exceed 2%, the  $M_{23}C_6$  carbide dominates. It is formed during heat treatment or is released during operation, usually at the grain boundaries in the temperature range of  $933$  K  $\div$   $1253$  K.  $M_6C$  carbide occurs inside the grains [25].

## 3. STUDYING THE BLADE COATING MICROSTRUCTURAL CONDITION

### 3.1. Surface roughness tests

One of the parameters, the value of which can change due to blade heating at different temperatures is surface roughness. It is

defined as a non-conformity or deviation from the product profile assumed in the drawing. This parameter is measured at small surface sections. It is described by two basic parameters:  $R_a$  and  $R_z$  [8]. The  $R_a$  parameter is privileged in testing and is most often measured. There is the  $R_z \approx 4R_a$  relationship between these parameters. The 2D assessment of the surface geometric structure was conducted in the blade ridge area, using a PGM-1C profilometer with a BS 1000-10-1 WAT head. To define the surface profile, its roughness in the form of profile ordinate arithmetic means ( $R_a$ ,  $R_z$ ) were determined.

A sample roughness profile measured on the ridge in the middle part of a new blade profile is shown in Fig. 2. Based on the obtained measurement data presented in the form of graphs (Figs. 3 and 4), the authors concluded that heating temperature increase entails a decrease in  $R_a$  and  $R_z$  roughness first for a temperature of 1223 K and 1323 K, followed by a clear increase of said parameters at a temperature of 1523 K.

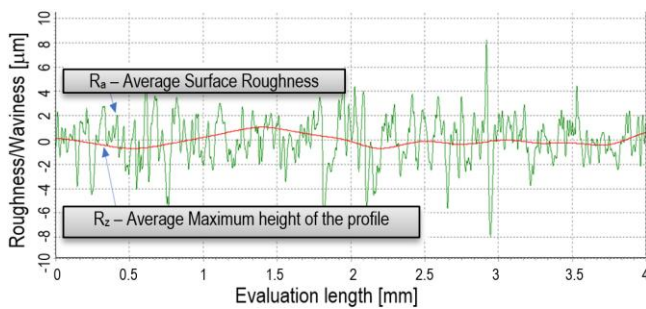


Fig 2. Sample roughness and undulation profile – new blade

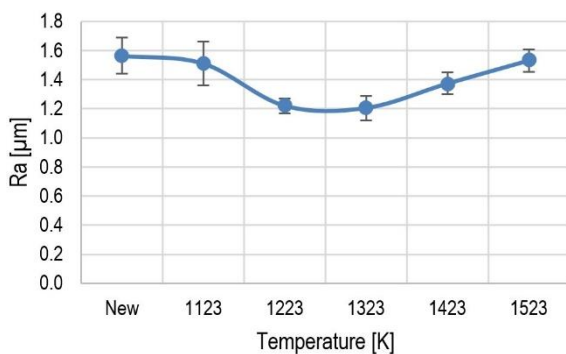


Fig. 3. Impact of heating temperature on roughness profile changes –  $R_a$

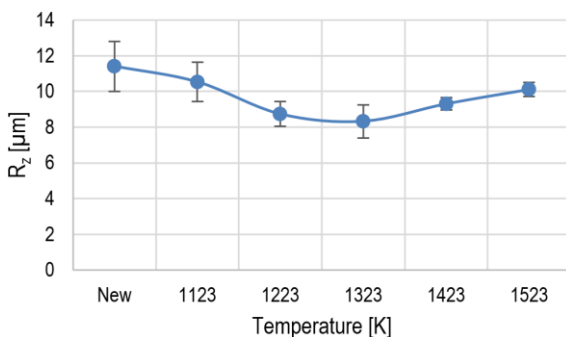


Fig. 4. Impact of heating temperature on roughness profile changes –  $R_z$

The recorded roughness changes directly translate to changes on the surface of the analysed blades under the influence of temperature and the environment. Based on the conducted microscopic examinations, chemical composition and surface distribution testing related to the elements, it was concluded that

scale made of an external aluminium, nickel and chromium oxide layer and fuel combustion products is formed on the surface of the described alloys.

### 3.2. Surface structure tests

The surface morphology of the analysed blades was tested and microstructural changes within the coatings were observed using a high-resolution scanning electron microscope Quanta 3D FEG. Quanta 3D FEG combines emission scanning electron microscope (SEM) with focused ion beam (FIB). It was concluded that scale was formed on the surface, leading to very significant morphological changes (imaging of surface topography using backscattered electrons (BSE) and topographic separation (BSE-TOPO)) - Figs. 5 ÷ 10. The surface of the new blade is relatively undeveloped with few defects in the scale formed on it. Cracks and delamination of the scale were observed in a few areas. As the heating temperature increases, on the one hand, the scale increases, which causes its delamination and, consequently, falling off. In this case, the morphological changes of the surface are caused by coagulant oxides forming on the scale surface, especially visible in Fig. 8b. A further increase in temperature only accelerates this process, causing the scale to fall off and, as a consequence, the native material is exposed (compare Fig. 5 with Fig. 10). It was found that increasing heating temperature on the surface of the analysed blades leads to the formation of, mainly,  $Al_2O_3$  and NiO oxides (Fig. 11). They form a surface layer protecting against further oxidation. The  $Al_2O_3$  oxide has a morphologically heterogeneous structure and a tendency to uneven growth and exfoliation, which reduces roughness at higher heating temperatures. Furthermore, there were areas observed on blade surfaces that are highly rich in carbon and sulphur, the presence of which is directly associated with aviation fuel components. The most undesirable aviation fuel component in this case is surface layer sulphur, which can occur in free or bound form (e.g., sulphides, disulphides, hydrogen sulphide and other). Furthermore, it was found that sulphur-enriched areas have products of partial or complete fuel combustions, e.g.,  $SO_2$ ,  $SO_3$ ,  $H_2S$ , etc., which cause the formation of sulphides based on the coating material.

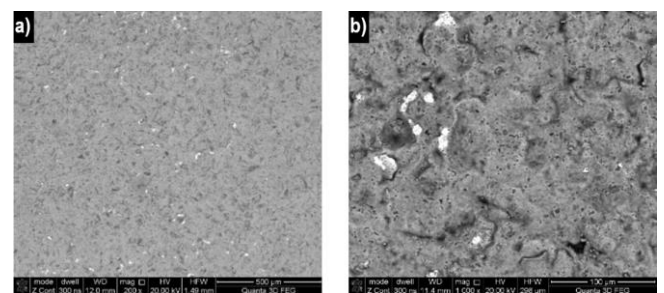


Fig. 5. Blade surface morphology - new, not heated: a) BSE-TOPO; b) BSE

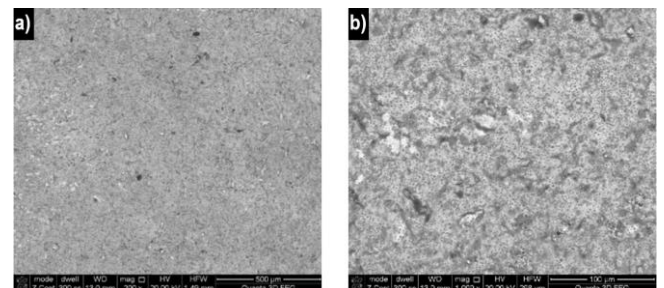


Fig. 6. Blade surface morphology at 1123 K: a) BSE-TOPO; b) BSE

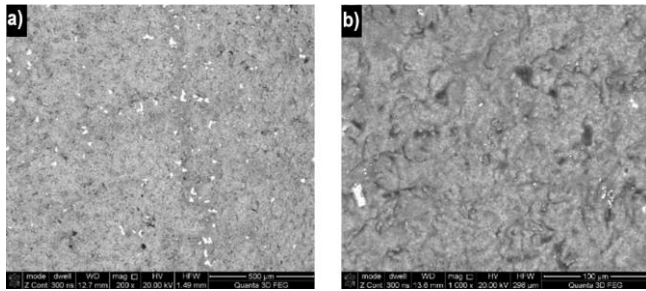


Fig. 7. Blade surface morphology at 1223 K: a) BSE-TOPO; b) BSE

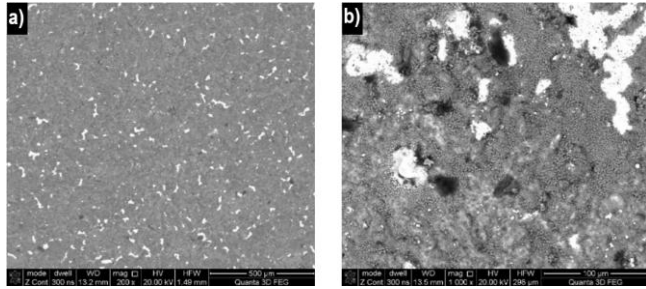


Fig. 8. Blade surface morphology at 1323 K: a) BSE-TOPO; b) BSE

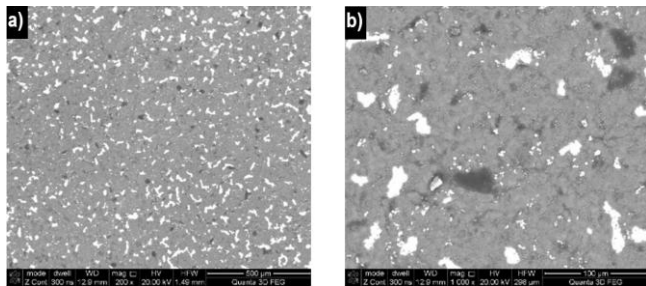


Fig. 9. Blade surface morphology at 1423 K: a) BSE-TOPO; b) BSE

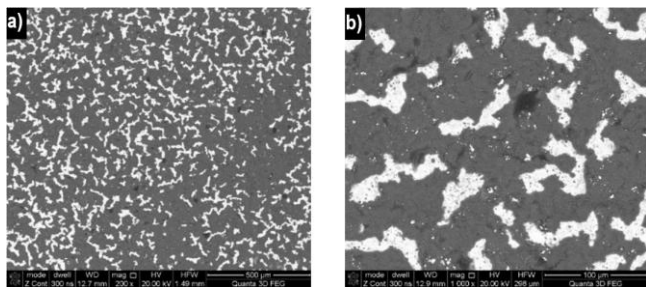


Fig. 10. Blade surface morphology at 1523 K: a) BSE-TOPO and b) BSE

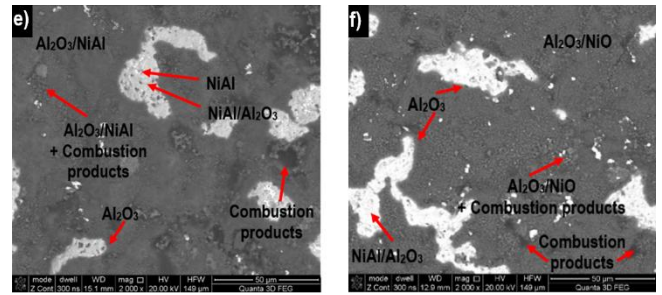
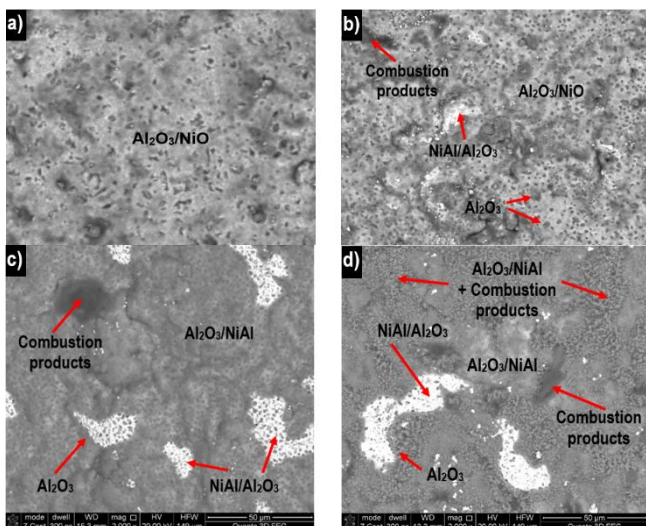


Fig. 11. Blade surface morphology: a) new; b) 1123 K; c) 1223 K; d) 1323 K; e) 1423 K; f) 1523 K

### 3.3. Area share of elements and oxides

Recorded structural changes ongoing on the surface of the analysed blades under the impact of temperature lead to very significant difference in the chemical and phase composition. It was found, among others, that a blade heating temperature increase results in considerable changes in the content of individual surface elements, primarily oxygen, chromium, nickel and carbon (Fig. 12-13). The observed changes are confirmed by independent EDS (Energy Dispersive Spectroscopy) and element mapping testing.

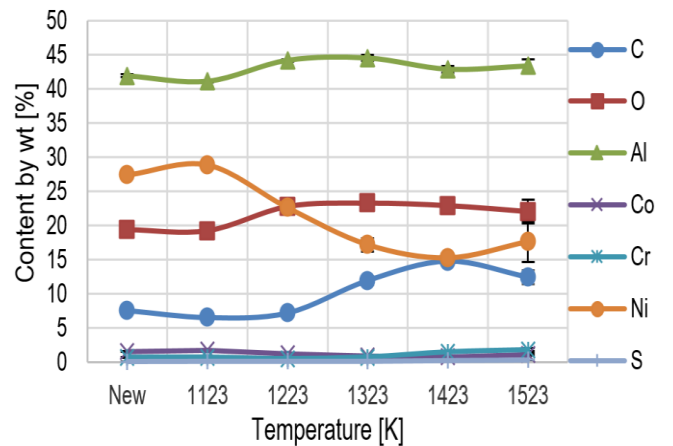


Fig. 12. Percentage share by weight of elements on the surface of tested blades – (SEM/EDS)

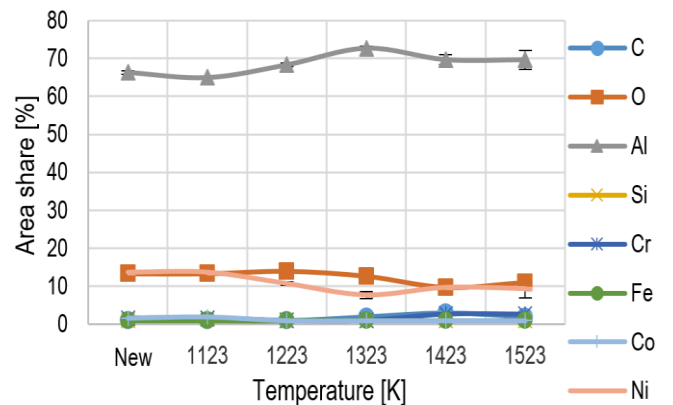


Fig. 13. Percentage share of elements on the surface of tested blades – element mapping method

Changes in the content of individual elements also translate to phase changes. They are particularly emphasized if we analyse the impact of temperature on the percentage content share of oxides on the surface of tested blades (Fig. 14). Based on the obtained data, it can be clearly seen that with increasing temperature, the mass oxide share reaches its maximum for a blade heated at 1423 K. In this case, the total oxide share exceeds 50% of the weight content. Furthermore, the recorded changes in oxide share directly translate to changes in their type. The impact of temperature on nickel oxide share changes is particularly noticeable in this case (Fig. 15). NiO content share changes impacted by temperature are primarily associated with the creation of the Al<sub>2</sub>O<sub>3</sub> scale on the surface of the analysed blades.

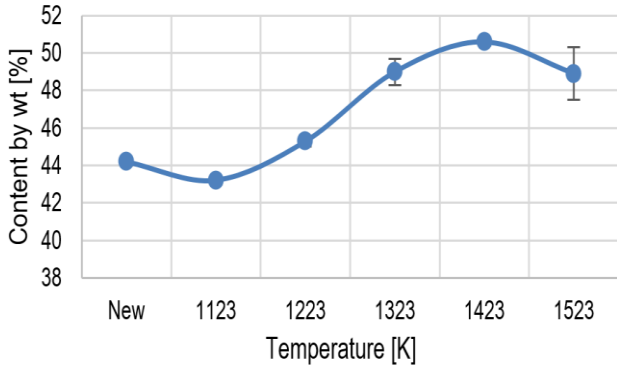


Fig. 14. Total percentage share of oxides measured on the surfaces of tested blades

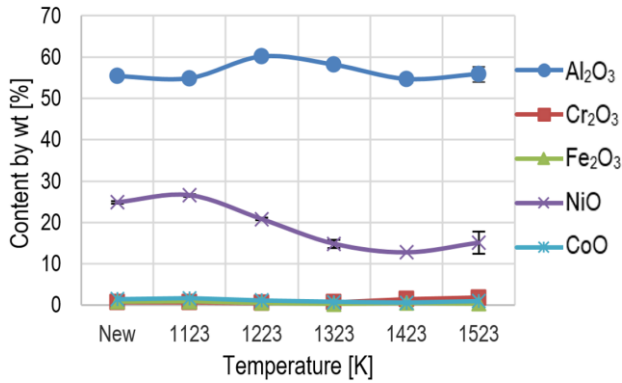


Fig. 15. Percentage share of individual oxides measured on the surfaces of tested blades

### 3.4. Microstructural tests

Thickness measurements were conducted using computer software for processing and analysing images from a Quanta 3D FEG microscope. Coating thickness was measured at characteristic blade locations, i.e., its edge of attack, trough surface and blade ridge – both inside and near the blade vane profile trailing edge. This provided an averaged aluminium thickness layer for each recorded (analysed) image (Fig. 16). Measured coating thickness values of a new blade (not heated) and a blade heated at different temperatures are shown in Fig. 17.

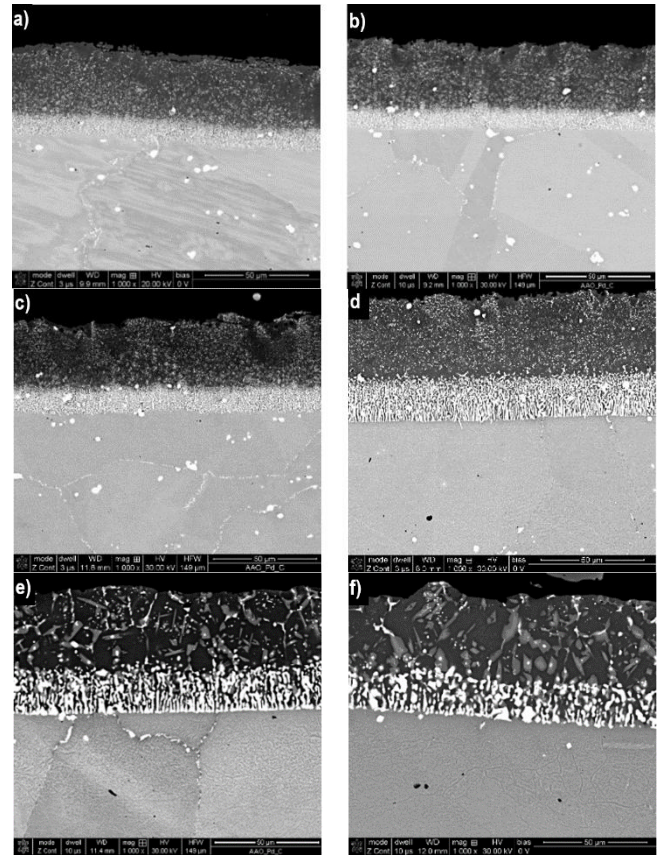


Fig. 16. Blade coating microstructures by heating temperature: a) new; b) 1123 K; c) 1223 K; d) 1323 K; e) 1423 K; f) 1523 K

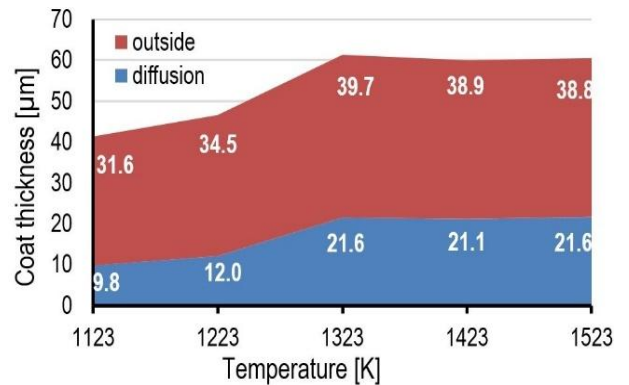


Fig. 17. Changes in the thickness of the external and diffusion coating exposed to different temperatures

### 3.5. Elemental composition of the internal and diffusion layers

The tests demonstrated that increased blade heating temperature leads to significant changes in the content of individual coating elements, nickel, chromium and aluminium in particular. Cumulative test results for a new blade and blades heated at 1123 K – 1523 K are shown in graphs (Figs. 18 and 19).

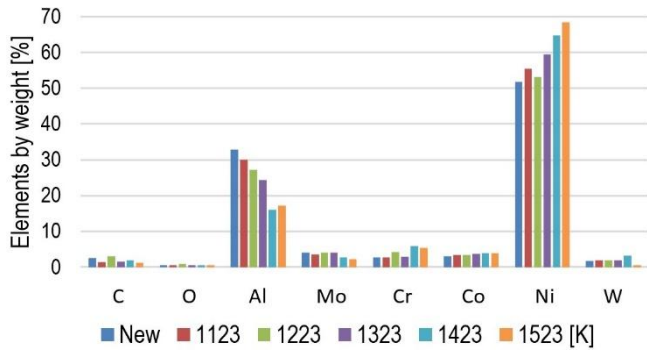


Fig. 18. Chemical composition of the external coating part of a new blade and heated blades

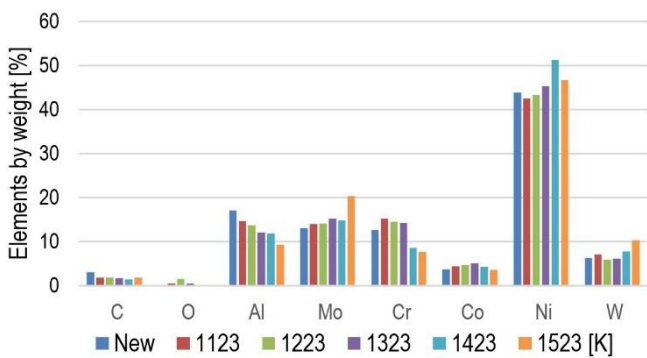


Fig. 19. Chemical composition of the diffusion coating part of a new blade and heated blades

#### 4. MICROSTRUCTURAL TESTS OF THE BLADE EI-867 WD ALLOY

##### 4.1. Grain size tests

Metallographic microsections were tested under a Nikon MA-200 optical microscope and a Quanta 3D FEG and XL30 LaB6 scanning (SEM) microscopes by Philips. Using NIS Elements AR material microstructure image analysis software, the authors determined the mean size (area) of the alloy grain and reinforcing phase  $\gamma'$ , expressed as the diameter of a circle with an area equal to the surface area of the measured object ( $Eqdia = \sqrt{4 \cdot Area / \pi}$ ). Images depicting alloy grain size by heating temperature can be seen in Fig. 20, and a change in its average size as a heating function can be seen in the graph in Fig. 21.

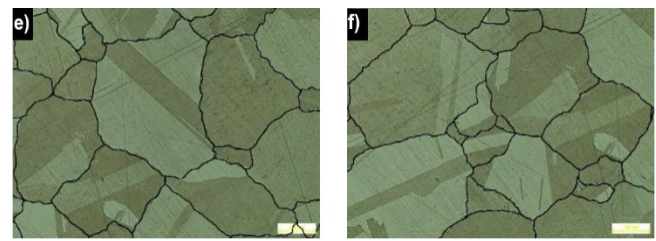
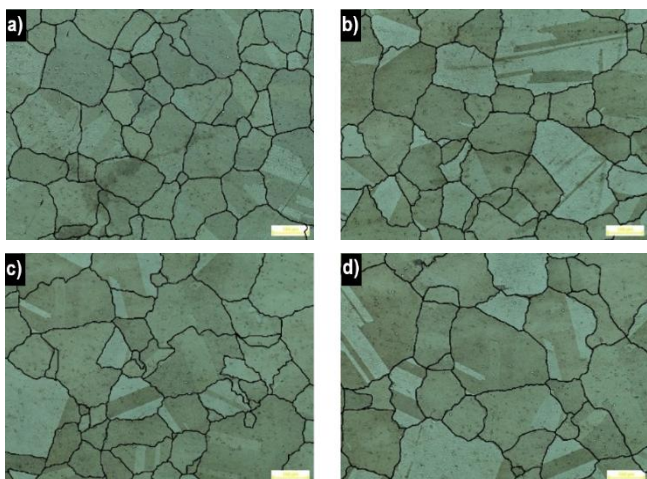


Fig. 20. Blade alloy grain size by heating temperature: a) new; b) 1123 K; c) 1223 K; d) 1323 K; e) 1423 K; f) 1523 K

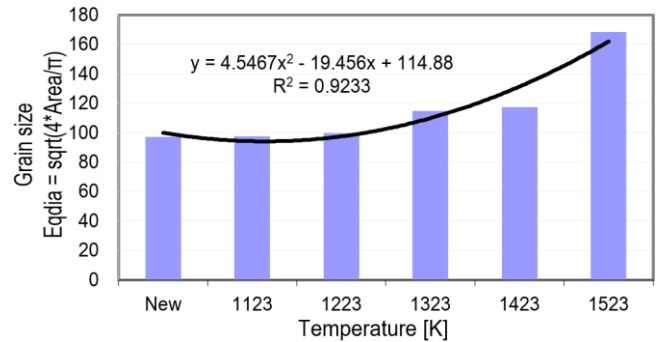
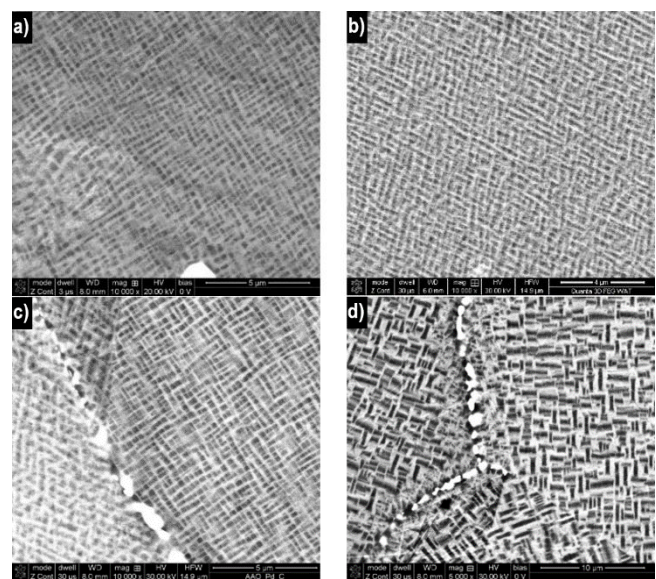


Fig. 21. The dependence of a change in the average blade alloy grain size on heating temperature, expressed by an equivalent diameter of a circle with an area equal to the grain surface area

##### 4.2. Reinforcing $\gamma'$ phase and carbide precipitate tests

The presence of carbides, even in a non-heated blade, can be observed in the alloy microstructure. Carbide content increases during heating, especially on grain boundaries. Carbides are stand-alone and in the form of "Chinese writing". A change in the  $\gamma'$  precipitate morphology was also found. The exposure of turbine blade alloy to high temperature also impacted their microstructural change, leading to a modification and distribution of the dispersive  $\gamma'$  phase. Fig. 22 shows sample images of microsections demonstrating the phase  $\gamma'$  precipitate morphology and the presence of stand-alone carbides. Based on analysing the microsections, the authors calculated a percentage content of individual phase  $\gamma'$  size classes in the blade alloy (Fig. 23) and the content of average-sized precipitates of this phase (Fig. 24).



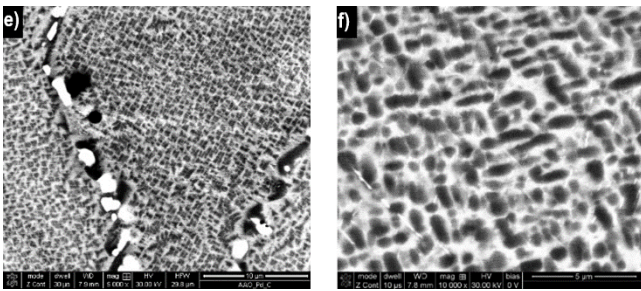


Fig. 22. Blade alloy phase  $\gamma'$  precipitate morphology by heating temperature: a) new; b) 1123 K; c) 1223 K; d) 1323 K; e) 1423 K; f) 1523 K

In the course of heating, the reinforcing  $\gamma'$  phase experiences significant changes, and its structure is modified (Fig. 23). A temperature of 1123 K favours the growth of phase  $\gamma'$  particles.

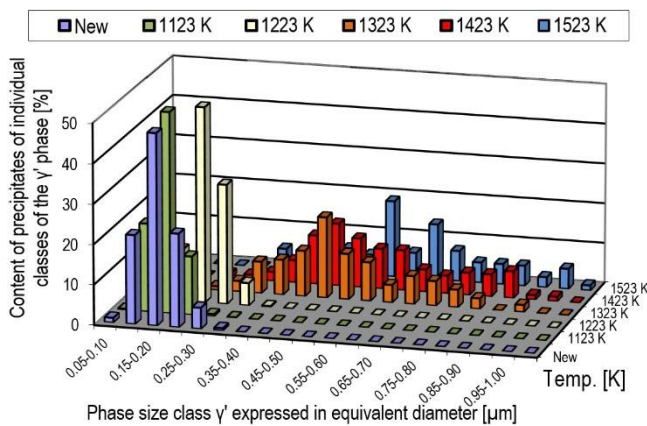


Fig. 23. Percentage precipitate content of individual phase  $\gamma'$  molecule size classes in the alloy

The average size of this phase molecules increases at a temperature of 1323 K (Fig. 23, Fig. 24). While at 1423 K, due to coagulation, the molecules with the largest initial dimensions increase (Fig. 23, Fig. 24).

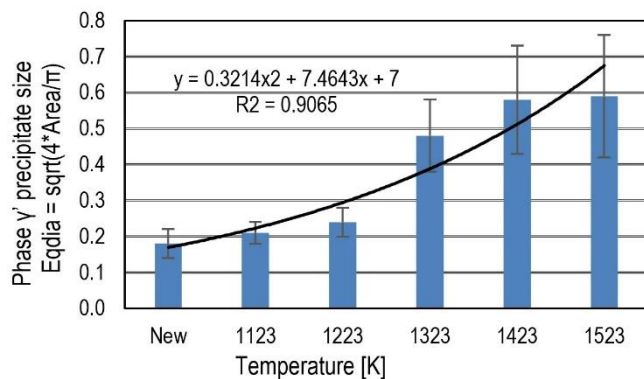


Fig. 24. Dependence of the average phase  $\gamma'$  precipitation in the alloy

It was found that temperature increase entails a reduction in the number of molecules with the largest dimensions relative to material microstructure changes in a new blade and a blade heated at 1123 K (Fig. 23). An increasing distance between  $\gamma'$  phase molecules is simultaneously seen. The observed growth, merging and wavy shape of the  $\gamma'$  phase particles are characteristic of an

overheated alloy and significantly reduce its heat resistance. Assuming the change in the phase  $\gamma'$  precipitate structure (Fig. 25) as a material criterion that enables further operation of the material, one can determine the suitability threshold for their further operation. According to the test results, after the temperature exceeds 1223 K and after an even relatively short exposure time, an intensive growth of the  $\gamma'$  precipitate occurs due to the bonding of fine-grained cubic phase  $\gamma'$  molecules into lamellas. This leads to the loss of cubic shape stability and the formation of irregular and undulated lamellas (Fig. 25).

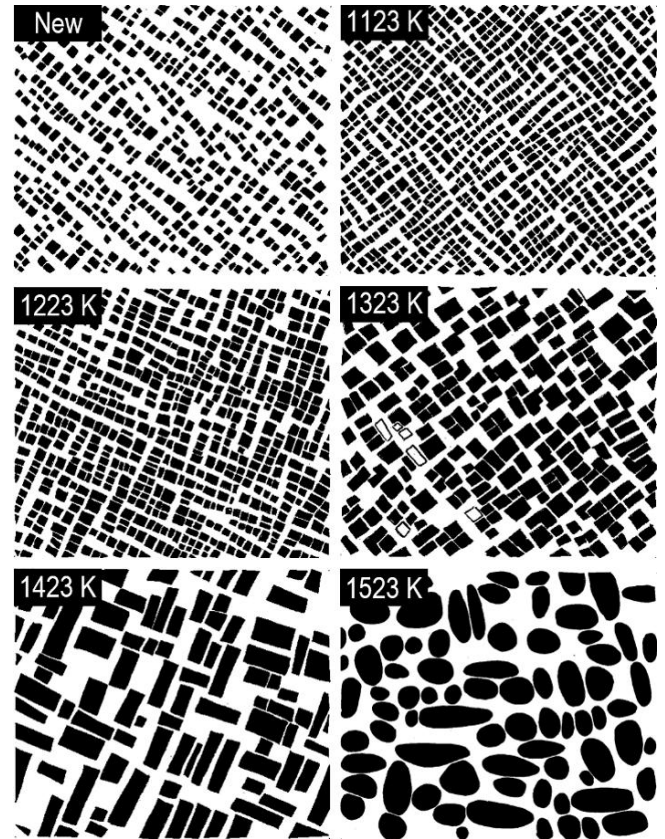


Fig. 25. Phase  $\gamma'$  precipitate microstructure of a new blade and heated blades (20000x zoom) – with visible coagulation, change of shape from cubic to irregular and phase precipitate undulation

## 5. DISCUSSION OF TEST RESULTS

In the course of the tests, it was found that coating surface morphology, as well as the chemical composition microanalysis spectrum and results indicate that these values significantly, and above all adversely, changed after heating. In the article [33] for the same material but under different experimental conditions, based on SEM/TEM studies in connection with the possibility of strengthening the physical basis of non-destructive testing of blades, microstructural processes occurring in the upper, most external layer of the coating were identified. It was found that above the temperature of 1223 K, a layer of aluminium oxide  $Al_2O_3$  is formed, the microstructure of the coatings is coarsened, pores are formed, Fe and Cr diffuse to the surface and Fe-Cr particles are formed and subsequently coarsened on the surface of the aluminium oxide layer. In the context of non-destructive inspection of blades exposed to high temperatures, the last process mentioned above is of particular importance, because it explains the changes in the light reflected from the blade surface.

The impact of increasing temperature causes the  $R_a$  and  $R_z$  roughness parameters initially decrease up to a temperature of 1223 K, followed by a slight increase up to 1323 K. The increase in  $R_a$  and  $R_z$  parameters is caused by the growing thickness of the heat-resistant coating, which considerably impacts the deterioration of its heat and corrosion resistance. Furthermore, various  $Al_2O_3$  and NiO oxides are formed on the blade coating surface together with increasing heating temperature. Aluminium oxide protects the coating surface against further oxidation. It has a morphologically heterogeneous structure and a tendency to uneven growth and exfoliation. Fluctuations in the parameters determining surface roughness are related to the processes of thermal softening, oxidation and microstructural changes. The presence of areas highly rich in carbon and sulphur was found on the coating surface. Their occurrence is directly associated with aviation fuel components. The most undesirable aviation fuel component is sulphur, which can occur in free or bound form of sulphides, disulfides and hydrogen sulphide. In the course of tests, the authors found that the total percentage share of oxides on coating surfaces initially grows, followed by a decrease at the highest heating temperature. The percentage weight share of the elements making up the coating is modified due to heating. A significant content difference can be seen, primarily in relation to the following elements: W, Mo, Ni and Al.

When testing the EI-867 WD alloy, it was found that MC carbides appeared when producing the blades in the alloy. They were found as stand-alone and in the form of "Chinese writing", mainly at grain boundaries. Carbides of such type can cause instabilities that reduce plasticity at low temperatures. The second of the identified carbides,  $M_6C$ , is more stable at higher temperatures. The  $M_6C$  carbide was mainly observed near grain boundaries. The next carbide,  $M_{23}C_6$ , precipitates during low-temperature heat treatment or in the course of alloy operation at temperatures from the 1033 K – 1253 K range. It is shaped as large, irregular precipitates at grain boundaries, in the form of lamellas or polygons. A  $M_{23}C_6$  carbide significantly impacts nickel-based superalloy properties. Grains grow in the alloy, which adversely impacts its mechanical properties. The observed transformation of  $M_{23}C_6$  carbides into  $M_6C$  in an alloy exposed to prolonged high temperatures (above 1223 K) is related to the diffusion of atoms, primarily molybdenum and tungsten present in the tested alloy, into the carbide structures. This high-temperature transformation from  $M_{23}C_6$  to  $M_6C$  leads to a decrease in creep resistance, as the process reduces the amount of stable reinforcing particles along the grain boundaries. Larger and less homogeneous  $M_6C$  carbides limit the alloy's ability to resist deformation under creep conditions. Additionally, the growth and transformation of carbides contribute to microstructural degradation, as  $M_6C$  carbides are less effective than  $M_{23}C_6$  in binding carbon at grain boundaries. This results in unfavourable changes in the alloy's microstructure, which in turn weakens its corrosion and oxidation resistance.

The expansion of the phase  $\gamma'$  particles leads to the loss of their stability, resulting in coagulation of some particles and dissolving of others. That process occurs above certain temperatures and heating time, characteristic for a given phase. According to the test results, after the temperature exceeds 1223 K and after an even relatively short exposure time, an intensive growth of the  $\gamma'$  precipitate occurs due to the bonding of fine-grained cubic phase  $\gamma'$  molecules into lamellas. This leads to the loss of cubic shape stability and the formation of irregular and undulated lamellas. This conclusion is also confirmed by the results in [34]. A similar conclusion was drawn by the authors of [25, 27, 35]. Based on the

example of the Udimet 700 alloy, lamellar-form precipitates above a temperature of 1093 K significantly deteriorate the yield strength. The kinetics of phase  $\gamma'$  precipitation depends on the supersaturation of the matrix, i.e., phase  $\gamma$ , with alloy elements. Exudation shape depends on the degree of mismatch between their grid with the warp grid. The authors of [34, 36] concluded that the precipitates of the  $\gamma'$  phase are coherent with the matrix, and the morphology is related to the degree of mismatch between phase  $\gamma$  and phase  $\gamma'$  lattice parameters. Furthermore, they found that the phase  $\gamma$ , with mismatch of the grid  $\Delta a = 0.2\%$  exudes in spheroid shape, at  $\Delta a = 0.5 - 1\%$  takes the cuboid form and at  $\Delta a = 1.2\%$  - tile form. A number of alloy properties depend on the phase  $\gamma'$  precipitate shape and amount. These include, e.g., the value of yield strength of weakening of adverse action of brittle phases – e.g., Laves. The exudation hardening theory shows that the factors deciding the hardening degree are diameter of phase  $\gamma'$  particles and distance between them. These parameters depend on the growth rate (controlled by volumetric diffusion) and coagulation of these molecules. Phase  $\gamma'$  chemical composition significantly impacts the value of its  $a_{\gamma'}$  lattice and the associated degree of mismatch between  $\Delta a$  and the  $a_{\gamma}$  lattice matrix. Wherein  $\Delta a = (a_{\gamma} - a_{\gamma'})/a_{\gamma}$ . This impact phase  $\gamma'$  precipitate morphology and its durability range. It turns out that the degree of mismatch of phase lattice parameters is a function of temperature. According to [34], the highest high-temperature creep resistance is exhibited by alloys with positive phase lattice mismatch. The chemical composition, morphology and microstructural arrangement of phase  $\gamma'$  precipitates have a decisive impact on alloy strength properties.

According to [25], the change in  $R_{0.2}$  and  $R_m$  strength properties for an analogous EI-867 alloy and for various test temperature values is of similar nature. A minor change in these two parameters is observed up to a temperature of 473 K. The value slightly increases up to approximately 673 K, followed by low fluctuation up until a temperature of ca. 1073 K, above which a clear reduction in tensile strength and yield strength can be seen.

## 6. PRACTICAL IMPLICATIONS OF THE FINDINGS AND THEIR LIMITATIONS

The tested turbine element, due to its core material, is classified as a nickel-based alloy, polycrystalline alloy with reduced chromium content and titanium-free. The lower chromium content requires the use of a coating – a coating that increases heat resistance properties and operating temperature by about 100 K. The tested object can be representative of a wide range of polycrystalline alloys with a similar chemical and volumetric composition of the  $\gamma'$  phase, which are used in heat exchangers, cooling systems or renewable energy systems. Certain findings, despite limitations resulting from tests conducted in laboratory conditions, have practical significance in relation to the group of alloys and coated materials characterized above:

- The  $\gamma'$  phase determines the mechanical properties of the alloy (durability of turbine blades).
- The microstructural modification of the  $\gamma'$  phase, carbides and grain boundaries depends on the temperature and time of its action and may constitute a parameter of the degree of microstructural degradation.
- Based on changes in the size of  $\gamma'$ , the approximate working temperature of the nickel alloy can be determined. The  $\gamma'$  phase precipitates change their size and shape during long-term

exposure to high temperature, which allows them to be used as indicators of the material's working temperature.

- In order to verify the technical condition of the blades, a comparative method can be used, in which the size and shape of the  $\gamma'$  phase of the new blade (standard values) are compared to the blade considered unfit for further operation during the technical inspection. On this basis, it can be stated, for example, that the damaged turbine blade (or superalloy in general) operated at an exhaust gas temperature above the maximum permissible temperature. Unfortunately, such tests are carried out using destructive methods. The proposed methodology for identifying damage to the gas turbine blade may prove helpful in the event of an engine failure, if the information on its operating conditions is insufficient.
- Diffusion processes (movement of aluminium from the interior of the coating to its surface) are more intensive the higher the temperatures. Additionally, long-term exposure to high temperatures leads to strong depletion of aluminium from the surface layer, which translates into a significant reduction in its resistance.
- Combustion products appear on the outer layer of the coating, and the presence of sulphur in exhaust gases intensifies corrosive processes. Sulphur reacts with aluminium, creating unstable compounds (e.g. sulphides), which weaken the coating and contribute to its degradation. Sulphur corrosion can lead to the formation of cracks and microcracks in the coating (acceleration of the coating degradation process). To some extent, combustion products affect the surface colour.
- Increase in coating thickness due to exposure to high temperatures is related to thermal expansion, phase changes and its oxidation. "Coating swelling" translates into a strong deterioration of its protective properties (in operating conditions, all destructive processes are intensified). Microstructural changes of the coating affecting the colour of its surface.

Several selected operational aspects that affect the limitations in formulating generalizations of the discussion of the results of the conducted laboratory experiment:

- Often, in real conditions, overheating of blades is local because the degree of impact of exhaust gases, thermal loads on the blade surface, is not uniform over the entire surface. The highest temperature values occur on the leading edge of the blade, because it is often accompanied by the process of stagnation of the exhaust gas temperature (dependence of the static value of the exhaust gas stream with defined thermodynamic properties and the flow rate value).
- The morphology of the  $\gamma'$  phase particles also depends on the sign of the mechanical stress. The tensile stress occurring axially of the blade during the rotation of the turbine rotor promotes the growth of the  $\gamma'$  phase in the plane perpendicular to the direction of stress. As a result, plates are formed from the original cuboid shape, the wider walls of which are located perpendicular to the direction of stress.
- There are several factors that increase the acceleration of the degradation processes of aluminium-based coatings. The working environment can be considered as particularly important. In coastal areas (even 40 kilometres from the reservoir) due to the increased concentration of chloride ions ( $\text{Cl}^-$ ), aluminized coatings are subject to accelerated degradation and destruction due to hot corrosion and oxidation. Under the influence of sea salts and high temperatures, they lose their protective properties. The coating loses thickness, which results in the gradual exposure of the basic blade

material, exposing it to further corrosion and operation at elevated temperatures despite the nominal operating conditions.

## 7. CONCLUSIONS

Gas turbine blades are exposed to high-temperature corrosion and cyclic thermal stresses, which lead to surface damage and thermomechanical fatigue. Prolonged exposure to this process, along with the adverse effects of elevated temperatures, causes blade overheating (significant microstructural degradation of the superalloy). Under operational conditions, this results in the formation of microstructural zones with locally diminished mechanical properties—namely, reduced heat resistance and creep resistance of the alloy. Excessively high temperatures relative to the nominal operating temperature, combined with tensile stresses during rotation, lead to creep in the superalloy. An important aspect of this issue is an attempt to determine the extent of modification in the state of the coating and the blade alloy material due to the effects of supercritical temperatures. Additionally, to approximate real conditions, the experiment was conducted in an exhaust gas environment. The research conducted could contribute to defining criteria for determining the suitability or unsuitability of the tested turbine element for further operation, based on information obtained through endoscopic devices without the need to dismantle the blades from the turbine. The technical condition of the blades can be indirectly assessed, i.e., based on the correlation between the light signal reflected from the coating surface (or, in its absence, the alloy surface) and the microstructural state of the alloy/coating.

The article describes the material changes (alloy and coating) in gas turbine blades of jet engines caused by high temperatures. Additionally, to simulate real conditions to some extent, the experiment was conducted in an exhaust environment. Microstructural studies performed, along with quantitative and qualitative results obtained, help in identifying significant material changes in both the coating and the alloy. They represent an attempt to comprehensively describe the material modifications in the blades (demonstrating differences compared to the material characteristics of a new blade). Section 6 presents practical implications of the results and certain limitations. The generalizations in this section attempt to point out potential applications in engineering practice while also considering certain limitations due to the experimental conditions and the interpretation of results in the context of real, complex working conditions of superalloys. The reflected light signal (colour) is influenced by factors such as the position and nature of the light source, as well as the surface roughness and chemical composition (see section 3). In terms of gas turbine blade durability, this material criterion is a decisive factor in defining strength properties (section 4 and discussion of results, see section 5).

1. Coating surface morphology, as well as the chemical composition microanalysis spectrum and results indicate that these values significantly changed after heating.
2. Due to the impact of increasing temperature, the  $R_a$  and  $R_z$  roughness parameters initially decrease up to a temperature of 1223 K, followed by a slight increase up to 1323 K. The increase in  $R_a$  and  $R_z$  parameters is impacted by growing thickness of the heat-resistant coating. Therefore, its heat and corrosion resistance deteriorates.
3. Various  $\text{Al}_2\text{O}_3$  and NiO oxides are formed on the blade coating surface together with increasing heating temperature.

Aluminium oxide has a morphologically heterogeneous structure and a tendency to uneven growth and exfoliation.

4. Furthermore, there are areas on blade surfaces that are highly rich in carbon and sulphur, the presence of which is directly associated with aviation fuel components.
5. The total percentage share of oxides on coating surfaces initially grows, followed by a decrease at the highest heating temperature. The percentage weight share of the elements making up the coating is modified due to heating.
6. There is little carbide presence when creating blades using the EI-867WD alloy, with the process dominated by the  $M_{23}C_6$  carbide, both in grains and at grain boundaries. The size and structure of the carbides changed in the course of heating, ultimately transforming into  $M_6C$ , and found primarily at grain boundaries.
7. Alloy grain growth was identified under the impact of high temperature, mainly above 1223 K.
8. The most significant microstructural changes were found in the precipitate morphology of the reinforcing  $\gamma'$  phase. The growth of molecules in this phase led to the loss of their stability.
9. The growth (adverse for heat resistance) and the percentage depletion of the reinforcing  $\gamma'$  phase in the alloy structure appeared at a temperature above 1223 K. This was caused by coagulation, a change of the shape from cubic to irregular and undulation of the reinforcing  $\gamma'$  phase precipitation.
10. The aforementioned changes in the microstructure of the EI-867WD changes led to significantly deteriorated strength properties in the course of heating at a temperature above 1223 K.

Further work will continue in the area of material characterization, focusing on single-crystal alloys and various types of coatings. On the other hand, diagnosing blades using videoscopes without removing them from the turbine remains challenging. The quality of the image obtained from the videoscope depends on the lighting and the device itself. Improper lighting settings, light reflections, or variable lighting conditions can affect the image coloration, which may lead to incorrect conclusions regarding the condition of the coating or the alloy surface.

## REFERENCES

1. Pollock TM, Tin S. Nickel-based superalloys for advanced turbine engines: Chemistry, microstructure, and properties. *J. Propuls. Power.* 2006; 22: 361–374.
2. Gudivada G, Pandey AK. Recent developments in nickel-based superalloys for gas turbine applications: review. *J Alloy Compd.* 2023;963.
3. Sims CT, Stoloff NS, Hagel WC. *Superalloys II-High-Temperature Materials for Aerospace and Industrial Applications.* New York (NY): John Wiley & Sons; 1987.
4. DeMasi-Marcin JT, Gupta DK. Protective coatings in the gas turbine engine. *Surf Coat Technol.* 1994;68:1–9.
5. Kadir A, Bég O, Gendy EIM, Bég TAB, Shamshuddin MD. Computational fluid dynamic and thermal stress analysis of coatings for high-temperature corrosion protection of aerospace gas turbine blades. *Heat Transf Asian Res.* 2019;48. doi:10.1002/htj.21493
6. Singh I, Tiwari AC. A revisit to different techniques for gas turbine blade cooling. *Mater Today Proc.* 2023.
7. Chowdhury TS, Mohsin FT, Tonni MM, Mita MNH, Ehsan MM. A critical review on gas turbine cooling performance and failure analysis of turbine blades. *Int J Thermofluids.* 2023;18:100329.
8. Hetmańczyk M, Swadźba L, Mendala B. Advanced materials and protective coatings in aero-engines application. *JAMME.* 2007;24:372–81.
9. Grimme C, Oskay C, Mengis L, Galetz MC. High temperature wear behavior of  $\delta$ - $Ni_2Al_3$  and  $\beta$ - $NiAl$  coatings formed on pure nickel using pack cementation process and diffusion heat treatment. *Wear.* 2021;477:203850.
10. Han J, Dutta S, Ekkad S. *Gas Turbine Heat Transfer and Cooling Technology.* New York (NY): Taylor and Francis; 2012.
11. Rajendran R. Gas turbine coatings—An overview. *Eng Fail Anal.* 2012;26:355–69.
12. Darolia R. Development of strong, oxidation and corrosion resistant nickel-based superalloys: critical review of challenges, progress and prospects. *Int Mater Rev.* 2018;64:355–80.
13. Azevedo C, Sinatora A. Erosion-fatigue of steam turbine blades. *Eng Fail Anal.* 2009;16:2290–303.
14. Laguna-Camacho JR, Villagran Y, Martínez-García H, Juárez-Morales G, Cruz-Orduña MI, Manuel VT, et al. A study of the wear damage on gas turbine blades. *Eng Fail Anal.* 2015;61:88–99.
15. Dubiel B, Moskalewicz T, Swadźba L, Czyrska-Filemonowicz A. Analytical TEM and SEM characterisation of aluminide coatings on nickel based superalloy CMSX-4. *Surf Eng.* 2008;24:327–31.
16. Carter TJ. Common failures in gas turbine blades. *Eng Fail Anal.* 2005;12:237–47.
17. Kopec M. Recent advances in the deposition of aluminide coatings on nickel-based superalloys: a synthetic review (2019–2023). *Coatings.* 2024;14:630. doi:10.3390/coatings14050630
18. Qu S, Fu CM, Dong C, Tian JF, Zhang ZF. Failure analysis of the 1st stage blades in gas turbine engine. *Eng Fail Anal.* 2013;32:292–303.
19. Kolagar AM, Tabrizi N, Cheraghzadeh M, Shahriari MS. Failure analysis of gas turbine first stage blade made of nickel-based superalloy. *Case Stud Eng Fail Anal.* 2017;8:61–8.
20. Belan J, Vaško A, Tillová E. Microstructural analysis of DV–2 Ni–base superalloy turbine blade after high temperature damage. *Procedia Eng.* 2017;177:482–7.
21. García-Martínez M, Del Hoyo Gordillo JC, Valles González MP, Pastor Muro A, González Caballero B. Failure study of an aircraft engine high pressure turbine (HPT) first stage blade. *Eng Fail Anal.* 2023;149:107251. doi:10.1016/j.engfailanal.2023.107251
22. Bogdan M, Błachnio J, Spychała J, Zasada D. Assessment of usability of the exploited gas turbine blade heat resistant coatings. *Eng Fail Anal.* 2019;105:337–46. doi:10.1016/j.engfailanal.2019.07.016
23. Villada JA, Bayro-Lazcano RG, Martínez-Franco E, Espinosa-Arbelaes DG, González-Hernandez J, Alvarado-Orozco JM. Relationship between  $\gamma'$  phase degradation and in-service GTD-111 first-stage blade local temperature. *J Mater Eng Perform.* 2019;28:1950–7.
24. Zhu J, An C, Lu Y, Zhu M, Xuan F. Research progress on effect of  $\gamma'$  phase on strength, fatigue and creep properties of nickel-based superalloys. *Mater Mech Eng.* 2023;7(6):1–7. doi:10.11973/jxgcc1202306001
25. Ponańska A. *Żywotność łopatek silników lotniczych ze stopu EI-867 w aspekcie odkształcenia niejednorodnego i zmian strukturalnych [doctoral dissertation].* Rzeszów: Rzeszów University of Technology; 2000.
26. Xiaotong G, Weiwei Z, Chengbo X, Longfei L, Stoichko A, Yunrong Z, Qiang F. Evaluation of microstructural degradation in a failed gas turbine blade due to overheating. *Eng Fail Anal.* 2019;103:308–18.
27. Skočovský P, Podrábský T, Belan J. Degradacja w wyniku eksploatacji warstwy aluminiowo-krzemowej łopatek turbinowych wykonanych na bazie Ni. *Archiwum Technologii Maszyn i Automatykacji.* 2004;24(1):45–52.
28. Mevissen F, Meo M. A review of NDT/structural health monitoring techniques for hot gas components in gas turbines. *Sensors.* 2019;19:711.
29. Kukla D, Kopec M, Sitek R, Olejnik A, Kachel S, Kiszowskiak Ł. A novel method for high temperature fatigue testing of nickel superalloy turbine blades with additional NDT diagnostics. *Materials.* 2021;14:1392.

- doi:10.3390/ma14061392
30. Bogdan M, Derlatka M, Błachnio J. Concept of computer-aided assessment of the technical condition of operated gas turbine vanes. *Pol Marit Res.* 2018;3(99):104–12. doi:10.2478/pomr-2018-0101
  31. Bogdan M, Błachnio J, Kulaszka A, Zasada D. Investigation of the relationship between degradation of the coating of gas turbine blades and its surface colour. *Materials.* 2021;14:2478. doi:10.3390/ma14247843
  32. Bogdan M, Błachnio J, Kulaszka A, Derlatka M. Assessing the condition of gas turbine rotor blades with the optoelectronic and thermographic methods. *Metals.* 2019;9:31.
  33. Bogdan M, Zieliński W, Płociński T, Kurzydłowski KJ. Electron microscopy characterization of the high temperature degradation of the aluminide layer on turbine blades made of a nickel superalloy. *Materials (Basel).* 2020;13:3240. doi:10.3390/ma13143240
  34. Paton B. *Żaropropczność litiejnych nikielowych spławów i zaszczuta ich ot okislenieja.* Kijew: Naukowa Dumka; 1997.
  35. Swadźba L. *Kształtowanie struktury oraz właściwości powłok ochronnych na wybranych stopach stosowanych w lotniczych silnikach turbinowych.* Katowice: Wydawnictwo Politechniki Śląskiej; 2007.
  36. Nikitin WI. *Korozja i zaszczuta łopatek gazowych turbin.* Leningrad; 1987.

This research was financed by the Ministry of Science and Higher Education of Poland with allocation to the Faculty of Mechanical Engineering Białystok University of Technology for the WZ/WM-IIM/4/2023 academic project in the mechanical engineering discipline.

Mariusz Bogdan:  <https://orcid.org/0000-0002-9960-7210>

Artur Kulaszka:  <https://orcid.org/0000-0002-8318-5877>

Dariusz Zasada:  <https://orcid.org/0000-0002-3138-5105>



This work is licensed under the Creative Commons BY-NC-ND 4.0 license.